Pressure variation prediction using seismic data for oil and gas exploration

Wildney W. S. Vieira, Boris P. Sibiryakov and Lourenildo W. B. Leite, UFPA, Brazil

Abstract

The present work is part of a major research study that has for objective the prediction of stress in sedimentary basins, as a contribution to geological and engineering methods and techniques for oil and gas exploration.

It is rather usual to think and to accept that pressure increases continuously with depth, and we show here that this is not the case. The vertical and horizontal pressure variations act as natural pumps that pushe fluids from high to low pressure zones. The major physical parameter for this phenomena is played by the $\gamma = \frac{v_S}{v_P}$ ratio discontinuity along interfaces.

Most of the seismic exploration is based on the acoustical wave equation, what results in a knowledge of the compressional wave velocity model. To obtain the shear wave velocity information it is necessary a 3D component sensor survey, and density log information can also be incorporated. Shear wave velocities can also be obtained from VSP technology, and by petrophysical measurements. There are tables and regression models for seismic velocities and densities that can also be incorporated in this prediction.

Introduction

This the prediction of subsurface stress and strain, and consequently pressure, use the P and S wave velocities ($v_P(\mathbf{x})$, $v_S(\mathbf{x})$) and density ($\rho(\mathbf{x})$) Sibiryakov et al. (2014b) and Sibiryakov et al. (2013).

The main question here raised is: How sensitive is the pressure prediction calculus to variations of velocity and density distribution.

The answer to this inquiry could be theoretically given by sensitivity analysis of the problem's differential equation system, or in a more practical way by numerical experiments. We chose this later route based on migration methodology, where testing is performed with smoothed versions of the input velocity model.

To develop the theory for stress-strain prediction for practical application in oil and gas exploration can be devide in three parts. The first part has to be related to conventional seismic investigations to obtain the P and S wave velocities and densities model. Also, the configuration of seismic boundaries in the sedimentary basins can be necessary. With these informations, the second part follows with the prediction of stress and strain, and of the nontrivial behavior of pressure. As a third part, is the continuation of the prediction of pressure discontinuity between solid and fluid, that depends on the structure of the pore space.

The data needed for pressure prediction can be 3C (three component sensors) to obtain P and S (SH and SV) wave modes, and density log information can also be incorporated. Also S wave velocities can also be obtained from VSP technology, and by petrophysical measurements (Hardage et al., 2011; Biondi, 2010; Galperin, 1985).

The theory is based on the static stress-strain equations, where the overload gravity weight is responsible for the strain and stress effects in the subsurface. Therefore, organizing this problem calls for Hooke's generalized law of linear elasticity.

It should be clear that here we are developing a specific data driven method that is based on $v_P(\mathbf{x})$, $v_S(\mathbf{x})$ and $\rho(\mathbf{x})$ knowledge, where we want to map low pressure zones important to locate a successful drilling zone for oil and gas exploration.

Methodology

The stress and strain tensor fields

The stress ($\sigma = \sigma(x,y,z)$) and strain ($\varepsilon = \varepsilon(x,y,z)$) elastic fields are related by the generalized Hooke's law, and described as tensors, functions of the space coordinates, and they are represented by nine components. Therefore, for the general anisotropic media the stress (σ) and strain (ε) tensors obey the spatial coordinate rotation relation given by:

$$\sigma_{ij} = \sum_{k,l} a_{ijkl}\sigma'_{kl}, \quad \text{and} \quad \varepsilon_{ij} = \sum_{k,l} b_{ijkl}\varepsilon'_{kl} \tag{1}$$

where the coefficients a_{ijkl} and b_{ijkl} define the new plane with respect to a reference system. The elastic linear relation between stress and strain is given by the generalized Hooke's law:

$$\sigma_{ij} = \sum_{k,l} c_{ijkl}\varepsilon_{kl}, \tag{2}$$

In this description, the first index (i) in σ_{ij} and ε_{ij} stands for the plane direction, and the second (j) for the component direction. As we particularize the stress state, it is represented at a point Q by a matrix $\mathbf{S}$, with the elements are σ_{ij}:

$$\mathbf{S} = \begin{bmatrix} \sigma_{xx} & \sigma_{xy} & \sigma_{xz} \\ \sigma_{yx} & \sigma_{yy} & \sigma_{xz} \\ \sigma_{zx} & \sigma_{zx} & \sigma_{zz} \end{bmatrix}. \tag{3}$$

Stress states

We now look at forms to represent the stress field. Therefore, turning to the stress matrix (3), it can be decomposed in three parts in the form: $\mathbf{S} = \mathbf{S_0} + \mathbf{S_D} + \mathbf{S_N}$, such that it allows for a physical interpretation (Persen, 1975). For the state $\mathbf{S_0}$ we have that:

$$\mathbf{S_0} = \begin{bmatrix} P_H & 0 & 0 \\ 0 & P_H & 0 \\ 0 & 0 & P_H \end{bmatrix}, \tag{4}$$

where

$$P_H = \frac{1}{3}(\sigma_{xx} + \sigma_{yy} + \sigma_{zz}), \tag{5}$$

with the sum (5) of the normal stresses in equation (4) defining the called hydrostatic pressure. This state is present in any plane around the point Q.

For the state $\mathbf{S_D}$ we have that:

$$\mathbf{S_D} = \begin{bmatrix} \sigma_{xx} - P_H & \frac{1}{2}(\sigma_{xy} + \sigma_{yx}) & \frac{1}{2}(\sigma_{xz} + \sigma_{zx}) \\ \frac{1}{2}(\sigma_{xy} + \sigma_{yx}) & \sigma_{yy} - P_H & \frac{1}{2}(\sigma_{yz} + \sigma_{zy}) \\ \frac{1}{2}(\sigma_{xz} + \sigma_{zx}) & \frac{1}{2}(\sigma_{zy} + \sigma_{yz}) & \sigma_{zz} - P_H \end{bmatrix}. \tag{6}$$

For the above equation (6), applying the symmetry property: $\sigma_{xy} = \sigma_{yx}$, $\sigma_{xz} = \sigma_{zx}$, $\sigma_{yz} = \sigma_{zy}$, $\mathbf{S_D}$ results in a null state; i. e., $\mathbf{S_D} = \mathbf{0}$.

For the state $\mathbf{S_N}$ we have that:

$$\mathbf{S_N} = \begin{bmatrix} 0 & \frac{1}{2}(\sigma_{xy} - \sigma_{yx}) & \frac{1}{2}(\sigma_{xz} - \sigma_{zx}) \\ \frac{1}{2}(\sigma_{xy} - \sigma_{yx}) & 0 & \frac{1}{2}(\sigma_{yz} - \sigma_{zy}) \\ \frac{1}{2}(\sigma_{xz} - \sigma_{zx}) & \frac{1}{2}(\sigma_{zy} - \sigma_{yz}) & 0 \end{bmatrix}. \tag{7}$$

Similarly, applying the symmetry property, the state $\mathbf{S_N}$ simplifies to:

$$\mathbf{S_N} = \begin{bmatrix} \sigma_{xx} - P_H & \sigma_{xy} & \sigma_{xz} \\ \sigma_{yx} & \sigma_{yy} - P_H & \sigma_{xz} \\ \sigma_{zx} & \sigma_{zx} & \sigma_{zz} - P_H \end{bmatrix}. \tag{8}$$

called the deviatory state for the diagonal elements (normal stresses), where the hydrostatic state is subtracted to remain the nonhydrostatic state.

From the above discussion, we posed physically the following stress field representation: the hydrostatic pressure state (5), and the deviatory state (8). But, still other representations are possible as seen in the sequel, and all of them must be adapted here for analyzing the 2D case. The simple word "pressure" (positive or negative) is here always related to the normal stresses.

Isotropic media

For an isotropic media, perfect linear elastic, the relation between stress and strain is given by Hooke's law in the form:

$$\sigma_{ij} = \lambda\theta\delta_{ij} + 2\mu\varepsilon_{ij}, \tag{9}$$

where λ and μ are the Lame's elastic parameters, and δ_{ij} Kronecker's delta ($\delta_{ij} = 0$, if $i \neq j$ and $\delta_{ij} = 1$, if $i = j$). The θ parameter represents the dilatation given by the divergence of the displacement vector $\vec{u}$ as:

$$\theta = \nabla \cdot \vec{u} = \frac{\partial u_x}{\partial x} + \frac{\partial u_y}{\partial y} + \frac{\partial u_z}{\partial z}. \tag{10}$$

The strain tensor components ε_{ij} are defined in terms of the displacement components u_i as:

$$\varepsilon_{ij} = \frac{1}{2}\left(\frac{\partial u_i}{\partial x_j} + \frac{\partial u_j}{\partial x_i}\right). \tag{11}$$

Also, the shear-extensional linear process produces a rotation tensor that is given by:

$$\varphi_{ij} = \frac{1}{2}\left(\frac{\partial u_i}{\partial x_j} - \frac{\partial u_j}{\partial x_i}\right). \tag{12}$$

Therefore, once we know the displacement vector components (u_i), the functionals quantities in equations (10), (11) and (12) can be calculated (Lowrie, 2011).

From the above discussion, for an isotropic media only two constants are necessary to completely specify the stress-strain relation. Boundary conditions are usually described by stress and strain relations (mixed boundary problem) across an interface, as continuity, free condition, and discontinuity. And to be specific, discontinuity is the case of a boundary condition along the contour of a reservoir, with the form of an anticline, or of a stratigraphic trap.

Since the model is related to the wave propagation in a perfect elastic medium, the elasto-dynamic equations of motion is resumed to the form:

$$\frac{\partial \sigma_{ij}}{\partial x_j} = \rho\frac{\partial^2 u_i}{\partial t^2}, \quad (i,j = 1,2,3); \quad \text{or} \quad (i,j = x,y,z). \tag{13}$$

That means that the spatial stress variation is related to the inertial force per unit volume, without internal forces (the gravity effect).

The velocities of the basic seismic body waves (P and S) in homogeneous, isotropic, elastic media are given by:

$$v_{\mathrm{P}} = \sqrt{\frac{K + \frac{4}{3}\mu}{\rho}} = \sqrt{\frac{\lambda + 2\mu}{\rho}} \quad \text{and} \quad v_{\mathrm{S}} = \sqrt{\frac{\mu}{\rho}}, \tag{14}$$

where K is the bulk modulus (the modulus of incompressibility), μ is the shear modulus (modulus of rigidity), ρ is the density of the material through which the wave propagates, and λ is related to K and μ.

From the above relations (14), the shear module is calculated by $\mu = v_{\mathrm{S}}^2\rho$, the Lambda module by $\lambda = v_{\mathrm{P}}^2\rho - 2\mu$, and the Gamma ratio by $\gamma = \dfrac{v_{\mathrm{S}}}{v_{\mathrm{P}}}$.

Now we turn to our differential equation system to be integrated, and this system represents the problem's description for the static system, where the time variation is null. In this case, the equations are resumed to the form:

$$\frac{\partial \sigma_{ij}}{\partial x_j} = \rho g \delta_{3j}, \quad (i,j = 1,2,3); \quad \text{or} \quad (i,j = x,y,z). \tag{15}$$

It means that the horizontal stress variations are considered null, and the vertical component is given by the gravity load in terms of force per unit area (ρg). Therefore, lateral tectonic stress is not here taken into consideration. The quantities ρ and g can be considered as spatial functions; i.e., $\rho = \rho(x,y,z)$ and $g = g(x,y,z)$.

We consider at first a simple model formed by a horizontally layered medium. The equation of equilibrium for the linear elastic medium for every single layer is given by:

$$\frac{\partial \sigma_{ik}}{\partial x_k} = \rho g_i, \tag{16}$$

where σ_{ik} are the components of stress tensor, ρ is the rock density, and g_i is the acceleration. For the case of vertical gravity, $g_{i=z}(z) = g$, it is taken as constant for a rather short depth, and a simpler equation (16) is written in the following form:

$$\frac{\partial \sigma_{zz}}{\partial x_z} = \rho g. \tag{17}$$

The above equation has an elementary solution given by:

$$\sigma_{zz}|_{z=z_0} = \int_{z=0}^{z=z_0} \rho g dz = \rho g z_0 = P_0(z_0), \tag{18}$$

where $P_0 = \rho g z_0$ is the weight of rocks per unit area; that is, the vertical pressure due to the overload at any depth z_0.

In the physical aspects of this theory, we do not take in consideration geological faulting and lithological variations for the rock volume forming the reservoir. Also, in another paper we deal with the case of bending of the geological formation resulting in an anticline structure (Sibiryakov et al., 2014a).

Scalar pressure field

The pressure field in rocks is a main characteristic of the stress condition of the geological structures. Stress is nonhydrostatic even in horizontal layered media subject to only vertical gravity compaction without horizontal displacement. Lateral tectonic stress is, therefore, a condition to be explicitly considered in organizing the model.

For the present simplified model, the vertical stress, $\sigma_{zz}(z)$, is defined as equal to the weight of the overburden; i. e.:

$$\sigma_{zz} = P_z = P_0(z). \tag{19}$$

The horizontal stress, $\sigma_{xx}(z)$, considering that $\sigma_{yy} = \sigma_{xx}$ in this case, is sufficiently lower than the vertical stress, σ_{zz}, and from equations (15) and (18), it is shown to be given by:

$$\sigma_{xx} = P_x = P_0(1-2\gamma^2), \tag{20}$$

where $P_0 = P_0(z)$, $\gamma = \gamma(z) = \frac{v_S(z)}{v_P(z)}$.

The scalar invariant hydrostatic pressure field, $P(z) = P_H$, was defined above as the average $P = P_H = \frac{1}{3}(\sigma_{xx} + \sigma_{yy} + \sigma_{zz})$. Using the generalized Hooke's law in the form (9), this field can be calculated by:

$$P = P_H = (\lambda + \frac{2}{3}\mu)\theta, \tag{21}$$

where $\theta(z)$ is the dilatation given by equation (10), and $\lambda(z)$ and $\mu(z)$ are the already described Lame's parameters.

Another important physical characteristic is the overburden pressure discontinuity at layer boundaries ($\Delta P = P^+ - P^-$, at z, and z positive downwards), that will exist if the velocity γ ratio has a discontinuity. Considering the simplest case of layered media, and Hooke's law (9), the discontinuity ΔP is given by:

$$\Delta P(z) = \frac{4}{3}(\gamma_1^2 - \gamma_2^2)P_0(z), \tag{22}$$

where γ_1 is the upper and γ_2 the lower layer parameters across the interface positioned at depth z. Therefore, overburden pressure varies stepwise as positive or negative with depth, if the underlying γ ratio is different from the overlying γ ratio. This idea may appear rather strange in simple geology, but it is an important fact related to the nonelementary behavior of stress in solids.

Results

The experiments were devided in two main parts based on the input data: (1) Original, and (2) Smoothed (v_P, v_S and ρ). The selected results for presentation had symmetrical smoothing operators with the following lengths: 41, 81, and 101 points.

The same smoothing process was equally applied to the input model components (v_P, v_S and ρ) to analyze the resolution decay of the prediction results. We focused on some reservoir targets, as the input parameters systematically deviate from the original (real) values. This means that we used the same criteria as in the numerical tests for stack, inversion and migration experiments.

The data selected and used for the present test was from the Marmousi seismic project (Versteege and Grau, 1991), and described by Martin et al. (2006) as we show in Figure 1, where we call attention to the gas an oil reservoir targets.

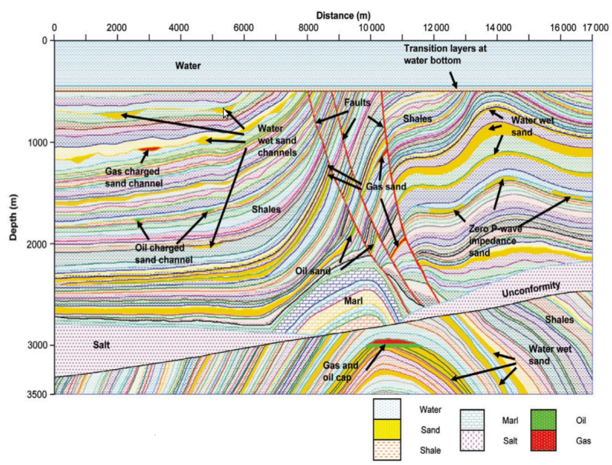

Figure 1: Geological description of the Marmousi according to Martin et al. (2006) with the oil and gas reservoir targets pointed to. We underlined the target in the bottom sequence related to the classical anticline structure.

Figures 2, 3 and 4 show the input v_P, v_S and ρ data, where the main aspects (low frequency) are still recognized, but the details (high frequency) have been very much attenuated with the smoothing process. Figures 5 and 6 show the γ and the Poisson ratios, $\sigma = \frac{1-2\gamma^2}{2-2\gamma^2}$.

One goal, based on description for this model by Versteege and Grau (1991), is marked with a rectangular window defined along the x-axis with the coordinates of $10.000-11.000$ meters, and in the z-axis by the coordinates of

$2.800-3.200$ meters. That is, the top of the anticline defined as an oil and gas reservoir. Therefore, this spatial window marks a confined low pressure zone representing the reservoir.

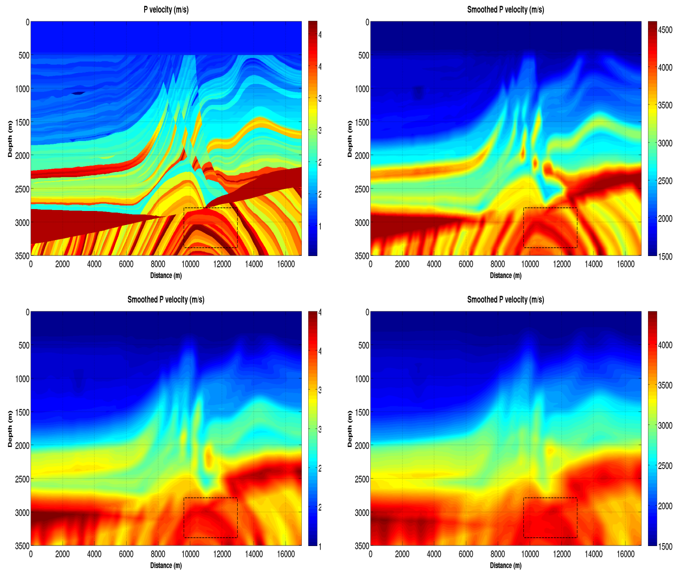

Figure 2: Velocity, $v_{\mathrm{P}}(x,z)$.

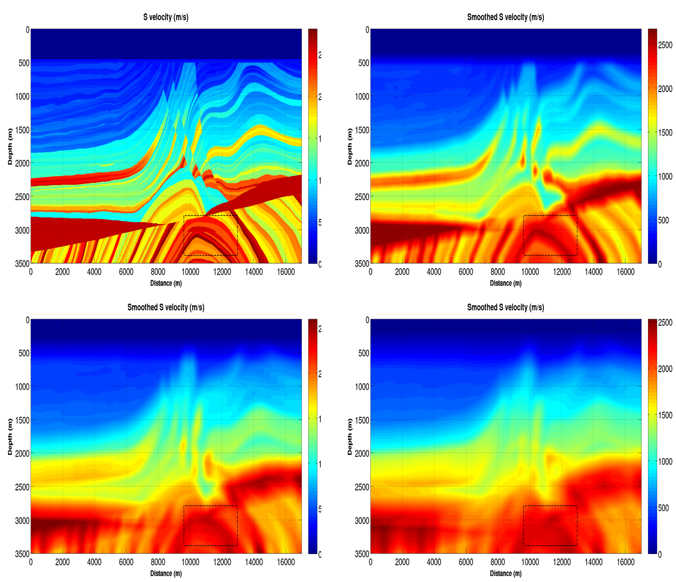

Figure 3: Velocity, $v_{\mathrm{S}}(x,z)$.

Figure 7 shows the vertical pressure field calculated by equation (19), and it displays a direct visual difficulty to identify reservoir structures as the smoothing increases.

Figure 8 shows the horizontal pressure field calculated by equation (20). This figure clearly still shows details of the target reservoir and of the geological structure as the smoothing increases, and it becomes one main conclusion of this study.

Figure 9 shows the hydrostatic pressure field calculated by equation (5) adapted to the 2D case as $P=P_H=\frac{1}{2}(\sigma_{xx}+\sigma_{zz})$, and it does not show details of the target reservoir in the geological structure as the smoothing increases, but a very smooth field expression.

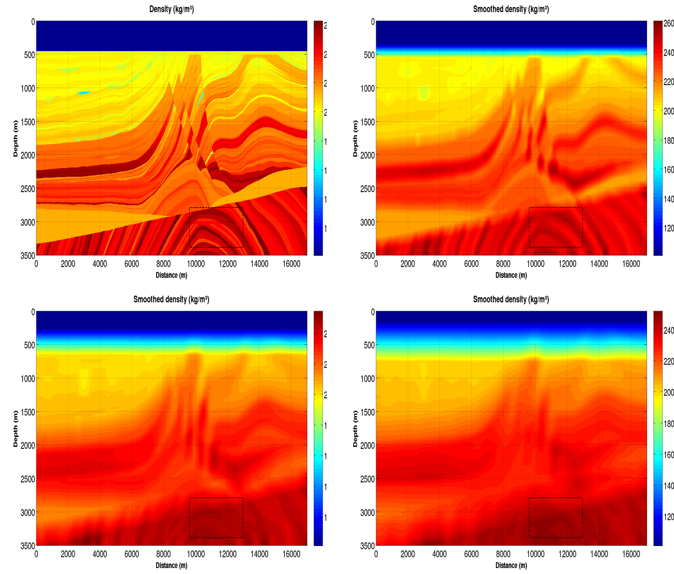

Figure 4: Density, $\rho(x,z)$.

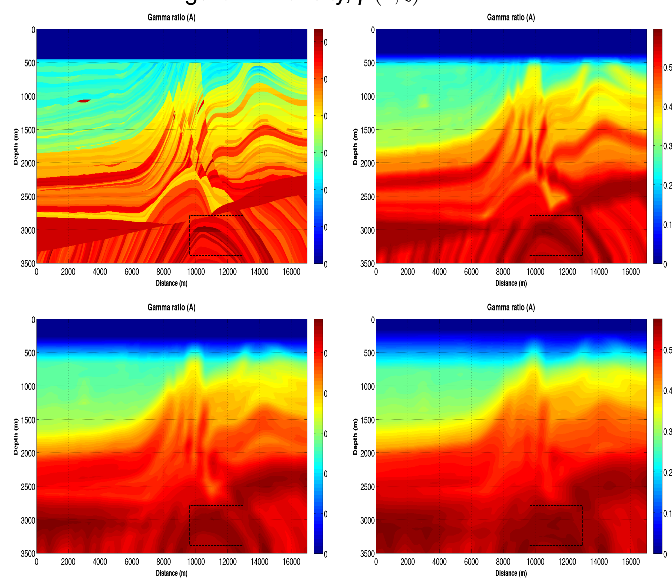

Figure 5: Gamma, $\gamma(x,z)$.

Figure 10 shows the horizontal deviatory hydrostatic pressure field, $P_{XH}=\sigma_{xx}-P_H$. Figure 11 shows the vertical deviatory hydrostatic pressure field, $P_{ZH}=\sigma_{zz}-P_H$.

Figure 12 shows the vertical pressure discontinuities calculated by equation (22). In this special figure, we can identify the geological sequences of the model, and it also shows clearly details of the target reservoir as the smoothing increases. This is also another important conclusion of these numerical experiments.

Conclusions

The conclusions are related to the main goal established by the initial question on how sensitive is the pressure

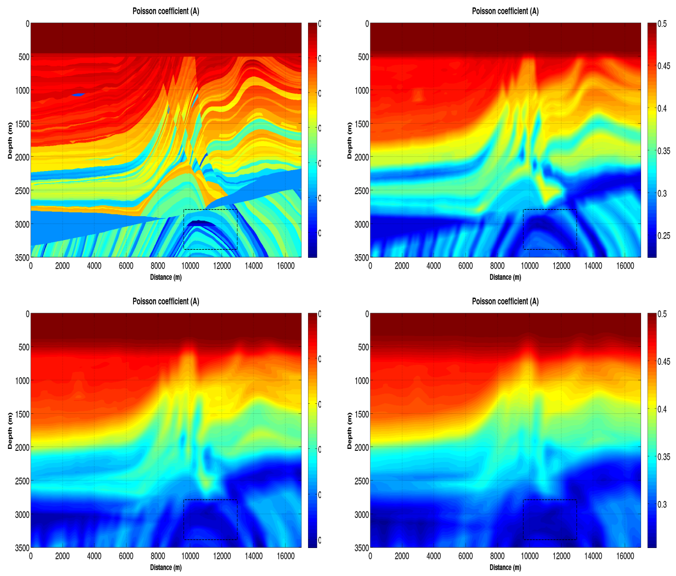

Figure 6: Poisson, $\sigma(x,z)$.

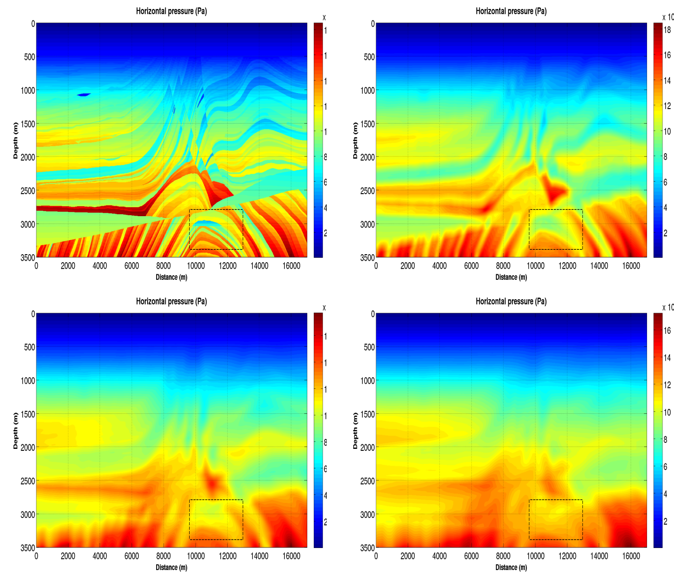

Figure 8: Horizontal pressure field, $P_x(x,z)$.

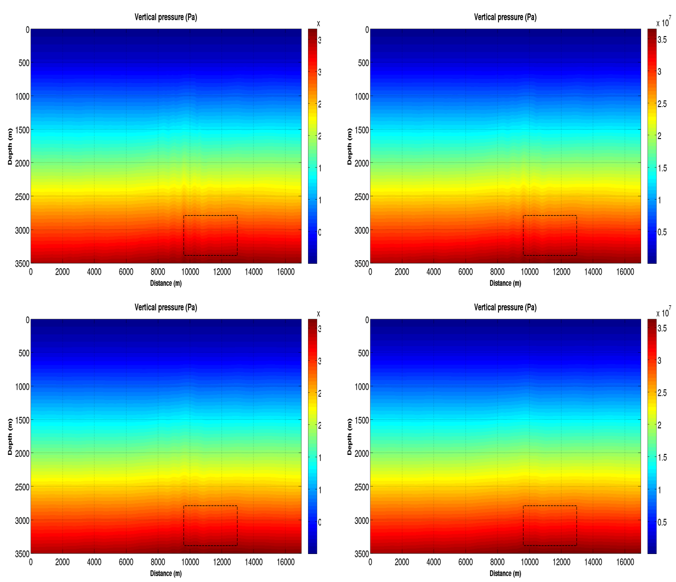

Figure 7: Vertical pressure field, $P_z(x,z)$.

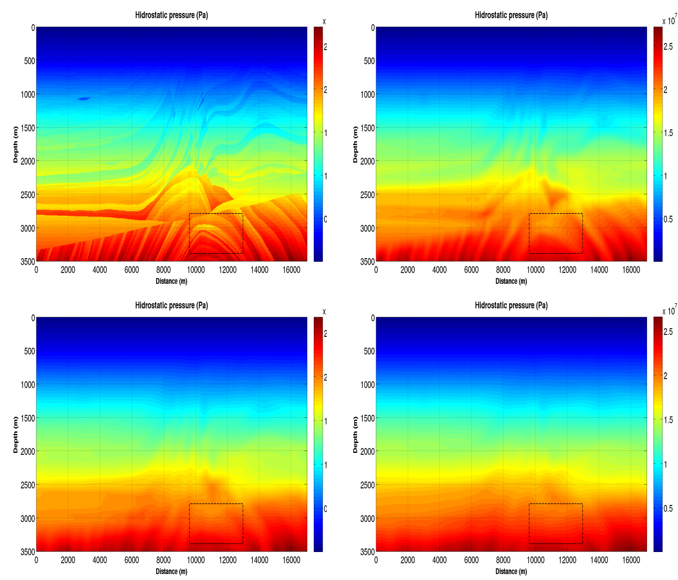

Figure 9: Hydrostatic pressure field, $P_H(x,z)$.

prediction to the variation of velocity and density, principally around a geological reservoir zone, with the results should be presented in the form of depth sections in the geological domain.

In situ measurement of stress is described to be very important in several fields of engineering, geology and geophysics aiming at several applications, and here we are concerned with oil and gas exploration.

We showed details of the calculus, and used an important example to show how pressure varies in the subsurface of the synthetic classical Marmousi model. In order words, we showed that pressure does not necessarily increases linearly, but in a complex form. The marked target by a spatial window defines a confined low pressure zone representing the reservoir, but other low pressure areas are also mapped.

As a detail, the theory limits the stress agent to be the vertical load of the geological rock formations, and does not take into account the reflector's curvatures, faulting and diagenesis.

Stress and pressure prediction is an important issue for the analysis of a sedimentary basins, aiming at oil and gas potentially productive areas

The sensitivity analysis to measure the decay in the resolution of the stress state prediction in this example followed the migration methodology. The horizontal pressure field in Figure 8 exhibits details of the target reservoir in the geological structure as the smoothing process increases, and it is one of the main results

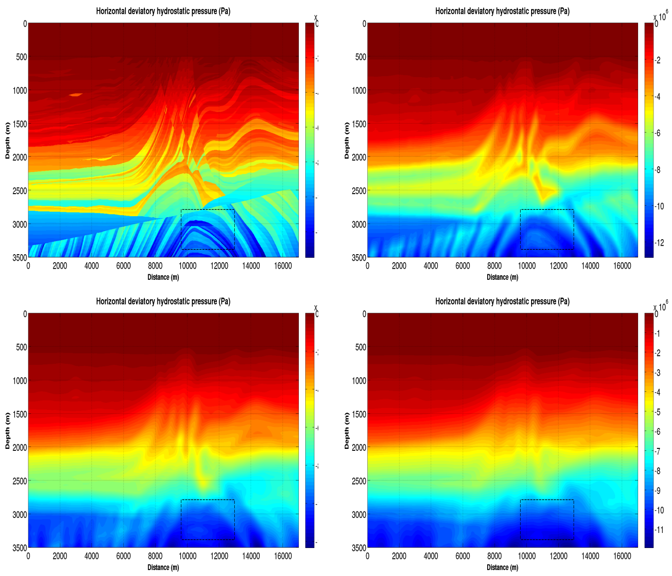

Figure 10: Horizontal deviatory hydrostatic pressure field, $P_{XH} = \sigma_{xx} - P_H$.

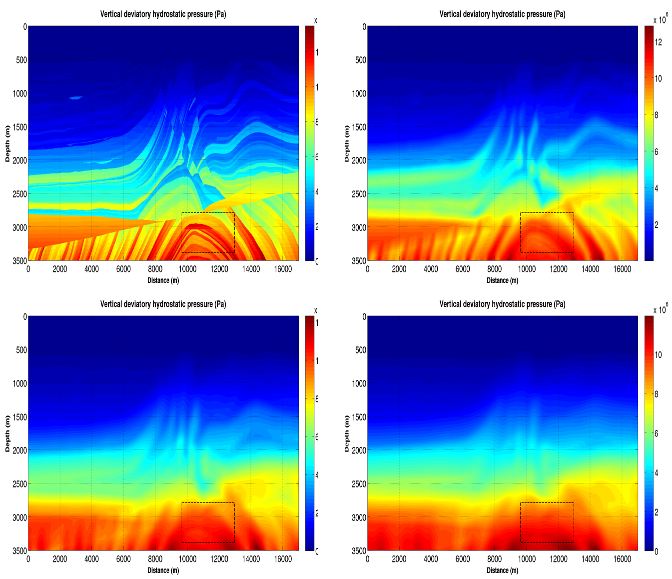

Figure 11: Vertical deviatory hydrostatic pressure field, $P_{ZH} = \sigma_{zz} - P_H$.

obtained here.

The vertical pressure discontinuities in Figure 12 allows the identification of the geological sequences, and clearly shows details of the target confined reservoir as the smoothing process increases. This is also a special result in this work.

References

Biondi, L. B., 2010, 3d seismic imaging: Society of Exploration Geophysicists, Tulsa, OK, USA.

Galperin, E. I., 1985, Vertical seismic profiling and its exploration potential: D. Reidel Publishing Company, Boston.

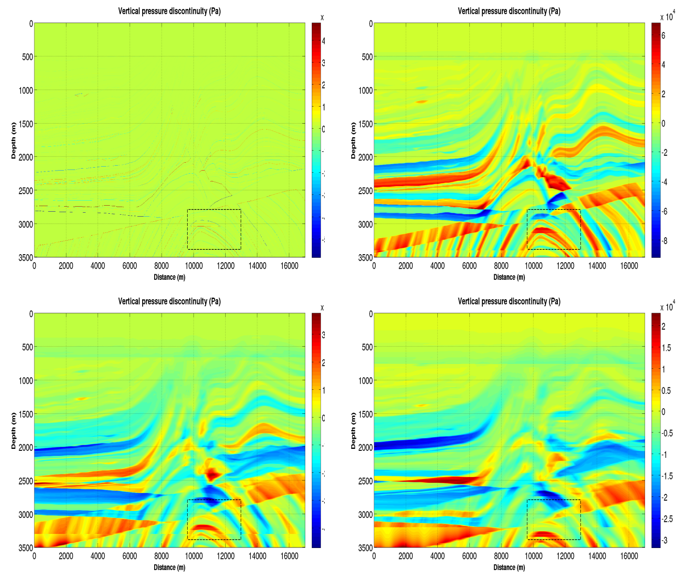

Figure 12: Vertical pressure discontinuities, $\Delta P(x,z)$, across the interfaces.

Hardage, B. A., DeAngelo, M. V., Murray, P. E., and Sava, D., 2011, Multicomponent seismic technology: Society of Exploration Geophysicists, Tulsa, OK, USA.

Lowrie, W., 2011, A student's guide to geophysical equations: Cambridge University Press, London.

Martin, G. S., Wiley, R., and Marfurt, K. J., 2006, Marmousi2: An elastic upgrade for marmousi: The Leading Edge. SEG., pages 156–166.

Persen, L. N., 1975, Rock dynamics and geophysical exploration: Elsevier Scientific Publishing Company, Amsterdam, Holland.

Sibiryakov, E. P., Leite, L. W. B., and Vieira, W. W. S., 2013, Model of the structured continuum, and the relation between specific surface area, porosity and permeability: Brazilian Journal of Geophysics, **31**, no. 4, 559–568.

Sibiryakov, E. P., Leite, L. W. B., Sibiryakov, E., and Vieira, W. W. S., 2014a, Local low pressure areas in anticline structures (accepted): Brazilian Journal of Geophysics.

Sibiryakov, E. P., Leite, L. W. B., and Vieira, W. W. S., 2014b, Behavior of stresses and hydrodynamics from multicomponent seismic data (accepted): Brazilian Journal of Geophysics.

Versteege, R. J., and Grau, G., 1991, The marmousi experience: Proc. EAGE Workshop on Practical Aspects of Seismic Data Inversion. Copenhagen.

Acknowledgments

The authors would like to thank the sponsorship of Project INCT-GP. Also to the Science Without Borders of CNPq/CAPES that has sponsorsed the major part of this research aiming at oil and gas exploration. Special to the Project PRH-06 that is present in this research. To the Project FINEP-Fase-5, and to CAPES for the scholarship.